IOP Conference Series: Materials Science and Engineering

Structure and properties of MgB_2 bulks: *ab-initio* simulations compared to experiment

To cite this article: V V Romaka *et al* 2020 *IOP Conf. Ser.: Mater. Sci. Eng.* **756** 012020

IOP Conf. Series: Materials Science and Engineering **756** (2020) 012020 doi:10.1088/1757-899X/756/1/012020

Structure and properties of MgB_2 bulks: *ab-initio* simulations compared to experiment

V V Romaka[1], T A Prikhna[2,9], M Eisterer[3], A P Shapovalov[2], W Goldacker[4], V E Moshchil[2], A Kozyrev[2], M Rindfleisch[5], M Tompsic[5], E E Hellstrom[6], G E Grechnev[7], V Sh Zhang[8], F Yang[8], Ch Li[8]

[1] Lviv Polytechnic National University, 12 Bandera Str., Lviv, 79013, Ukraine
[2] V. Bakul Institute for Superhard Materials of the National Academy of Sciences of Ukraine, 2, Avtozavodskaya Str., Kiev 07074, Ukraine
[3] Atominstitut, TU Wien, Stadionallee 2, 1020 Vienna, Austria
[4] Karlsruhe Institute of Technology (KIT), 76344 Eggenstein, Germany
[5] Hyper Tech Research, Inc., 539 Industrial Mile Road, Columbus, OH, USA
[6] Colledge of Engineering, University of Wisconsin-Madison, 247 ASC - Shaw Building, 2031 East Paul Dirac Dr, Tallahassee, FL 323, USA
[7] B. Verkin Institute for Low Temperature Physics of the National Academy of Sciences of Ukraine, Kharkov 61103, Ukraine
[8] Superconducting Materials Research Center, Northwest Institute for Nonferrous Metal Research, 710016, Xi'an, China

[9]Author to whom any correspondence should be addressed, e-mail: prikhna@ukr.net

Abstract. Analysis of XRD patterns by Rietveld refinement has been shown that the main phase of superconducting MgB_2-based bulk materials (with high level of superconducting characteristics) has AlB_2 type structure and near $MgB_{1.8\text{-}1.68}O_{0.2\text{-}0.32}$ stoichiometry. The materials demonstrated the critical current densities up to 0.9 – 0.4 MA/cm^2 j_c (at 0 - 1 T, 20 K); up to 15 T B_{c2} (at 22.5 K) and B_{irr} (at 18 K). The *ab-initio* simulation confirmed (1) benefits in binding energy and enthalpy of formation if stoichiometry of the solid solution is near $MgB_{1.75}O_{0.25}$; (2) energetic advantage in case if impurity oxygen present only in each second boron plane of MgB_2 cell while the first boron plane of the same cell stays pristine and location of substituted oxygen atoms in the nearby positions. Besides, the results of *ab-initio* modeling allow explanation of the tendency towards segregation of O-impurity in MgB_2 structure during synthesis or sintering, and formation of Mg-B-O inclusions or nanolayers (with MgO type of structure) which effect pinning. Calculated transition temperatures, T_c, for $MgB_{1.75}O_{0.25}$ occurred to be 23.3 K, while for MgB_2 it was 21.13 K only. Experimental T_c of the bulk materials was 35.7-38.2 K.

1. Introduction

MgB_2 is oxygen-free superconducting compound with hexagonal AlB_2 type of crystallographic lattice. It contains close packed Mg layers and graphene like B layers alternate along the c axis of the hexagonal unit cell. MgB_2 shows a complex bonding structure consisting of ionic interlayer bonding and covalent/metallic mixed in-plane bonding. Existence of two energy gaps was shown for MgB_2 [1, 2]. The XRD study demonstrates that the MgB_2-based materials usually contain MgB_2 phase and some

IOP Conf. Series: Materials Science and Engineering **756** (2020) 012020 doi:10.1088/1757-899X/756/1/012020

admixture MgO phase even if special atmosphere is used during preparation for avoiding oxidation, see for, example [3, 4], what can be explained by high affinity of Mg towards oxygen. Besides, the presence of other admixture phases such as MgB_4 (orthorhombic), MgH_2 and BN, etc. can be observed on XRD patterns [5]. But in MgB_2-based materials structures can be as well present dispersed inclusions of higher magnesium borides, MgB_x, with x>4 (as SEM and Auger study witnessed), which cannot be reveled by XRD on the background of MgB_2 reflexes. The unit cells of higher borides such as MgB_7 (orthorhombic), MgB_{12} (orthorhombic), MgB_{12} (trigonal), MgB_{17} (trigonal), MgB_{20} (trigonal) and Mg_2B_{25} (trigonal) are rather complicated, containing many atoms. The large number of atoms in their unit cells and low symmetries of the cells are resulting in many 'reflecting planes' which essentially reduce the intensities of the XRD reflections, as compared to those of the MgB_2 (i.e. from a simple hexagonal unit cell). Because of this the dispersed inclusions of the higher magnesium borides can be practically 'invisible' for a traditional XRD analysis [6].

The study of MgB_2-based materials structures (bulk, wires, and thin films) by scanning electron microscopy (with quantitative X-ray microprobe analysis) and Auger spectroscopy (with quantitative analysis) showed us presence of oxygen in superconducting materials matrices (in a small amount) and presence of oxygen-enriched dispersed separate inclusions or nanolayers in the matrices. So, no pure MgO (without presence of boron) and no pure MgB_2 (without presence of oxygen) were experimentally revealed. The SEM and Auger study was performed using a JAMP−9500F which combined SEM SEI, BEI, X-ray and Auger analyzers and allow investigating of non-oxidized surfaces because the construction of the microscope gives possibility to perform etching of 1×1 mm^2 square surfaces by Ar ions directly in the exploratory chamber and even build depth profiles of distribution of present elements. In contrary to X-ray microprobe analysis which allows to estimate quantity of elements in the volume of material which is not smaller than 1-3 μm in diameter, emanated Auger electrons are collecting from a very small volume (10 nm in diameter and about two lattice parameters in depth) and thus nanoobjects can be properly analysed quantitatively by Auger spectroscopy. Besides, Auger spectroscopy is very sensitive toward light elements and simultaneous presence of B, C, O and N is not the obstacle for correct investigations.

The results of Auger spectroscopy and SEM study [6] of MgB_2-based materials with high superconducting performances: highly dense bulks [5-8], wires [9, 10] and thin films [8], would benefit from *ab-initio* modelling of boron atoms substitutions by oxygen atoms to calculate transition superconducting temperature of energetically the most preferable solid solution $MgB_{2-x}O_x$. The present paper is generalising results of the *ab-initio* modelling. The obtained data can be a basis for interpreting the unusual electronic properties of MgB_2-based materials and the development of nano-engineering of these materials with record values of superconducting characteristics.

2. Experimental

The microstructure of the materials was characterized by a JAMP−9500F. XRD patterns were obtained by X-ray powder diffraction analyses and Rietveld refinement (using "PHILIPS X'pert" and Dron-3). The critical current densities, j_c, of the bulks and thin films were estimated from data obtained by an Oxford Instruments 3001 vibrating sample magnetometer (VSM) using the Bean model [11]. Certain inconsistencies which may arise between different measurement techniques [12, 13] do not influence the result and discussion presented in this work. The values of transition temperature, T_c, the upper critical magnetic field, B_{c2}, and the irreversibility field, B_{irr}, were estimated from resistivity measurements (90% and 10% of the resistivity just above the beginning of the transition) using the four probe technique in fields from 0 to 15 T. Transition temperature, T_c, was experimentally estimated by SQUID magnetometer as well.

The list and characteristics of the materials under the discussion synthesized by the authors are shown in Table 1. The numbers assigned to the samples are used through the paper.

In order to obtain an approximate picture for the electronic structure of $MgB_{2-x}O_x$ compounds we have carried out the *ab-initio* calculations for corresponding $2\times2\times2$ and $2\times2\times1$ supercells of the initial MgB_2 unit cell to model various oxygen concentrations of the solid solution. The calculations were

Table 1. List and characteristics of film, wires and bulk materials.

No	Material	Initial materials	Preparation*	T_c, K
1	Wire	B (without C) and Mg – Specialty Materials Inc. (SMI)	One filament, 0.83 mm in diameter, Nb surrounding and	37.5
2	Wire	B (with C) and Mg (SMI)	monel outer sheath	31.6
3	Film	hot pressed MgB_2 target	Magnetron sputtering, 140 nm film thickness	33.5 (‖*ab*) 32.6 (‖*c*)
4	Bulk	Mg:2B (SMI)	2 GPa, 600 °C, in BN, HP	35.7
5	Bulk	Mg(chips):2B (0.66 wt. % O)	2 GPa, 1050 °C, in BN, HP	-
6	Bulk	Mg(chips):2B (0.66 wt. % O)+10% SiC	2 GPa, 1050 °C, in BN, HP	-
7	Bulk	Mg(chips):2B (1.4 wt. % O)	2 GPa, 900 °C, in BN, HP	38.2
8	Bulk	Mg(chips):2B (1.4 wt. % O)	50 MPa, 1050 °C, in C, SPS	37.5
9	Bulk	Mg(chips):2B (1.4 wt. % O)	30 MPa, 900 °C, in BN, HotP	37.1
10	Bulk	Mg(chips):2B (1.4 wt. % O)	0.1 MPa, 800 °C, in Ar flow	38.1

* HP- high pressure-high temperature conditions; HotP- hot pressed; SPS-spark plasma sintering.

based on the density-functional theory (DFT) and performed by employing the full potential linearized augmented plane waves (FP-LAPW) methods implemented in WIEN2k [14] and Elk [15] implementations) and the full-potential linear muffin-tin orbital (FP-LMTO) implemented in RSPt [16, 17]).

The exchange-correlation potential was taken into account in the local density approximation (LDA) [18] and the generalized gradient approximation (GGA) [19] of DFT. For the used full potential FP-LAPW and FP-LMTO methods any restrictions were not imposed on charge densities or potentials of studied systems that is especially important for anisotropic layered structures. The constructed supercells were based upon the experimental lattice parameters of the hexagonal MgB_2 cell, a_0=b_0=0.3086 nm; c_0=0.3524 nm. For the unit cell 1×1×1, supercells 2×2×1 and 2×2×2 the lattice parameters a, and c are considered equal to a_0 and c_0, 2a_0, and c_0, 2a_0 and 2c_0, respectively. In order to determine stable optimized positions of atoms and the related binding energies E_b in the $MgB_{2-x}O_x$ supercells, we applied the FP-LAPW method [14] within DFT-GGA approximation. The phonon calculations were performed within the Elk code (DFPT) for the optimized structure of $MgB_{1.75}O_{0.25}$ and the calculations of the superconducting critical temperature were conducted within Eliashberg theory using the formula [20] with the LDA [18] approach. In order to introduce oxygen in the initial MgB_2, the symmetry was reduced and the supercell 2x2x1 along the ab-plane was constructed. The scheme of MgB_2-2×2×2 supercell and the detailed descriptions of binding energy calculations as well as electronic structure variation of MgB_2 doped with oxygen are given in [21].

3. Results and discussions

Figure 1 shows the typical microstructures (after etching of their surfaces by Ar ions in the chamber of research microscope) of MgB_2 thin film (figure 1a, No 3 in table 1) wire (figure 1b, No. 1, manufactured by HyperTech from Mg and B without C addition,) and bulks synthesized from Mg:2B (amorphous) mixtures (figures 1c-f): in Ar flow at 800 °C (figure 1c, No10); at 1050 °C and quasihydrostatic 2 GPa pressure (figure 1d, No 5); at 1050 ^{0}C under 50 MPa pressure by spark plasma sintering (figure 1e, f, No 8). The differences in colors correlate with variation in concentration of magnesium, boron and admixture oxygen. The big darken gray areas in figure 1e connected with presence of MgB_4 phase (the pressure 50 MPa was not enough to suppress fully Mg evaporation during synthesis at 1050 °C). The materials superconducting characteristics (j_c, B_{c2} and B_{irr}, T_c) and XRD are presented in figure 2. The variation of stoichiometry on nanolevel has been observed (as difference in colors and microprobe quantitative analysis are shown) and the boundaries between areas with different concentration of elements (figure 1) can be responsible for pinning and high critical current density in MgB_2-based materials (figure 2). The data for the best samples synthesized under

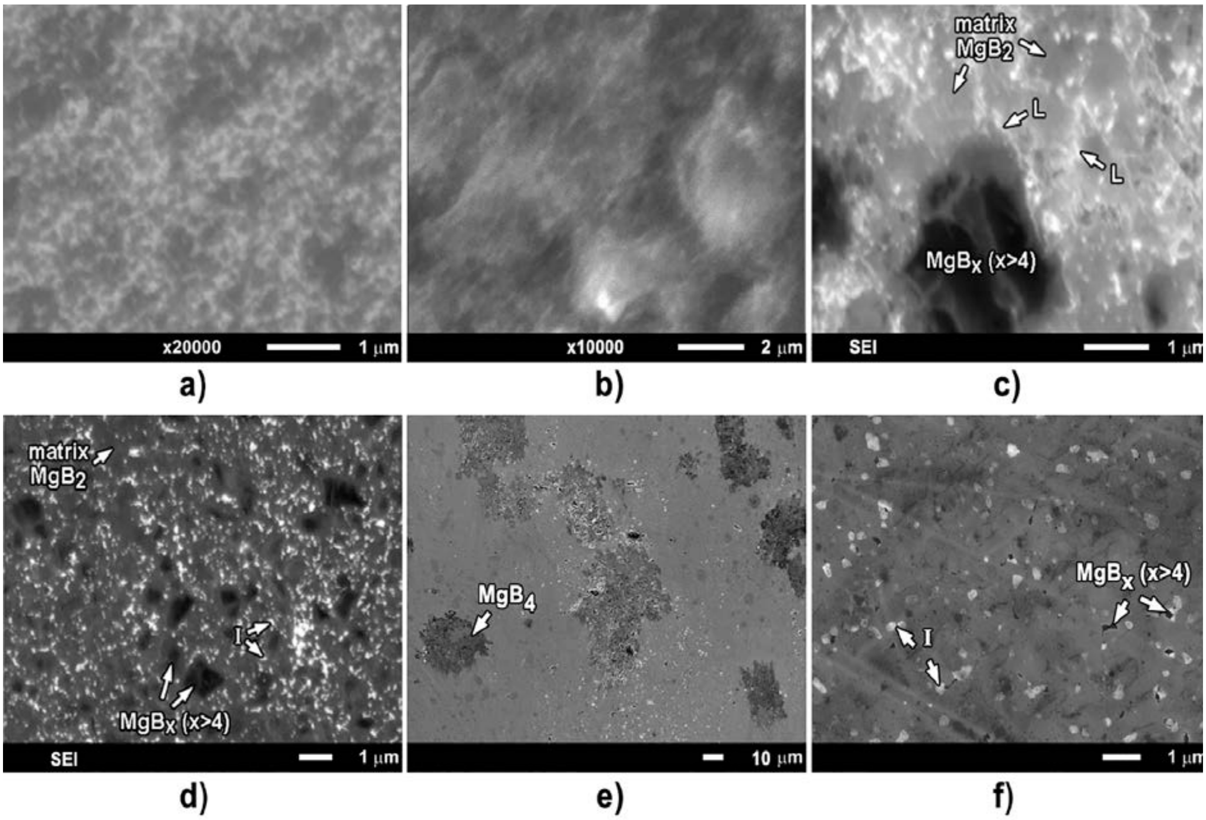

Figure 1. Typical microstructures of MgB_2 film No3 (a), wire No1 (b), and bulks: No 10 (c), No5 (d), No8 (e, f); numbering is according Table 1. All the materials contain B, Mg, admixture O and some small amount of admixture C; the brighter colors at the images correspond to lower concentration of boron and higher concentration of oxygen. By "I" and "L" the O- enriched inclusions and nanolayers, respectively, are marked.

each conditions (high pressure, HP, hot pressure, HotP, spark plasma sintering, SPS, or in Ar flow) are presented here.

Table 2 presents the results of Rietveld refinement of two samples: (1) prepared in protective from oxygenation atmosphere "with purified B" demonstrating T_c= 38.9 K [3] (figure 2g) and (2) synthesized under high pressure, No5 (table 1, figures. 2c, h). The temperature dependences of B_{c2} and B_{irr} for the material prepared "with purified B" are given in [3] (at 20 K its B_{c2} =8.8 T and B_{irr}=7 T). The results of Rietveld refinement (table 2) show $MgB_{1.8}O_{0.2}$ and $MgB_{1.74}O_{0.26}$ stoichiometries for the main phases present in the analyzed materials. The analysis of ten XRD patterns of MgB_2 materials with high superconducting performances showed $MgB_{1.8\text{-}1.68}O_{0.2\text{-}0.32}$ stoichiometries of their main phases. The XRD analysis of the diffraction pattern (figure 2h, table 2) showed the presence of 3 phases: the main phase MgB_2 and two impurity phases – BN and MgO. The Rietveld refinement revealed the presence of 5.6% on BN, 4.8% of MgO and the rest – 89.6% of MgB_2. In the case of the fully ordered MgB_2 phase with Mg solely occupying 1*a* (0 0 0) site and B occupying 2*d* (1/3 2/3 1/2) site the residuals between the calculated and experimental powder patterns were R_I = 2.96%, R_p = 9.77%, and R_{wp} = 14.0%. All attempts to refine the isotropic displacement parameters (B_{iso}) led to systematically high values for Mg atoms and very low (even negative) for B atoms. For this reason, two other models of the crystal structure were tested. The second model was refined with vacancies in the crystallographic site of Mg atoms. This led to somewhat lower residual R_I = 2.20% with 93.6% occupancy of the 1*a* site by Mg atoms. The third model was based on the statistical mixture of B and O atoms in 2*d* crystallographic site. The refinement of the third model revealed the lowest residual among three tested models: R_I = 1.92% and the 2*d* site occupied by 87% of B atoms and 13% of O

IOP Conf. Series: Materials Science and Engineering **756** (2020) 012020 doi:10.1088/1757-899X/756/1/012020

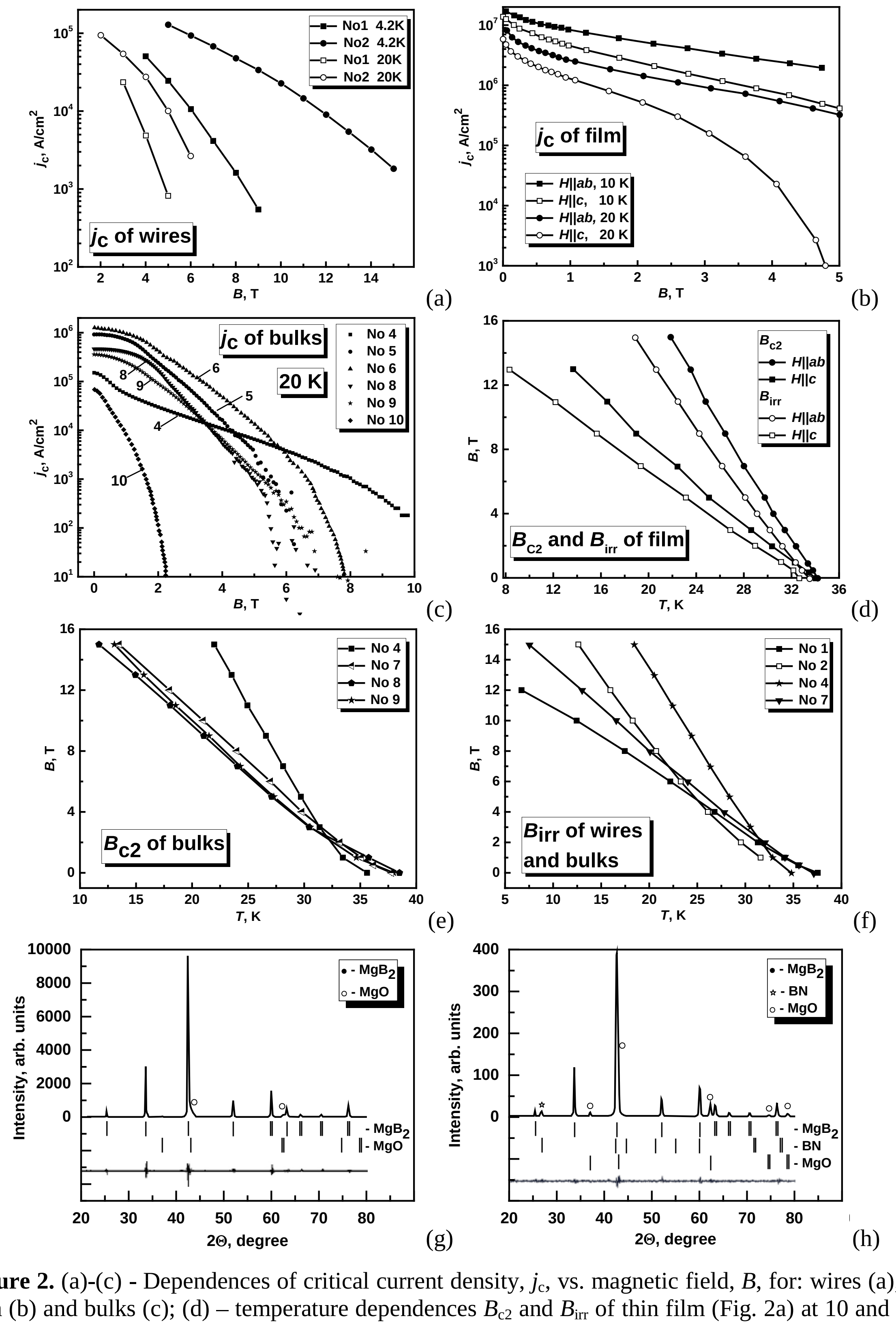

Figure 2. (a)-(c) - Dependences of critical current density, j_c, vs. magnetic field, B, for: wires (a), thin film (b) and bulks (c); (d) – temperature dependences B_{c2} and B_{irr} of thin film (Fig. 2a) at 10 and 20 K in two directions: parallel to the substrate surface (||*ab*) and perpendicular (||*c*); (e), (f) – temperature dependences of B_{c2} and B_{irr} of bulk and wires; (g), (h) – XRD patterns of MgB_2 bulks made in clean from oxygen conditions (the details are given in [1]) and of No5 (table 1).

Table 2. Results of Rietveld refinement.

Sample	MgB_2 (figure 2g), Ref.[3]	MgB_2 (Table 1 No 5, figure 2h)
Space group, structure type	*P*6/*mmm*, AlB_2	
a, *c* (nm)	0.30848(1), 0.35235(1)	0.30849(4), 0.35227(6)
Mg in 1*a*	0, 0, 0	
B_{iso} (10^2 nm^2)	0.36(5)	0.4(2)
B/O in 2*d*	1/3, 2/3, 1/2	
B_{iso} (10^2 nm^2)	1.11(7)	1.4
Occupancy B/O	1.80(2)/0.20(2)	1.74(2)/0.26(2)
R_I (%)	1.27	1.92
R_p (%)	7.60	9.65
R_{wp} (%)	11.4	13.9
Additional phases	MgO (1.9%)	BN (5.6 %), MgO (4.8 %)

giving the formula $MgB_{1.74}O_{0.26}$. All three models were tested with DFT calculations to compare their heats of formation, and the third model appeared to be the most energetically favorable. The analysis of XRD powder pattern of another bulk sample (figure 2g) showed that the sample contained only 1.9% of MgO impurity phase and the rest was MgB_2. Rietveld refinement was performed using the fully ordered model of MgB_2 and the model with B and O mixture in 2*d* site. The fully ordered model produced R_I =6.30%, while the model with B and O mixture – R_I = 1.27%. The refined oxygen and boron content in 2*d* site appeared to be very close to the first sample: 90% of B and 10% of O, which led to the formula $MgB_{1.80}O_{0.20}$.

For the DFT calculations we used the 2x2x2 supercell to model for the whole extent of dopant content (from 6 to 50 at% of substituting oxygen atoms). By means of FP-LAPW GGA calculations we optimized positions of atoms in the supercell from energetic point of view by method of step-by-step variation of the coordinates of all atoms. The criterion of optimization was taken as 0.001 Ry for energy variations. The results of the binding energies (E_b) calculations for oxygen substitutions were reported in Ref. [21] (see table 4). The analysis of the data has shown that the binding energy for almost all calculated $MgB_{2-x}O_x$ supercells is higher than that of pristine MgB_2. If we impose restriction to consider the high symmetric cells only, the monotonous increase of binding energy can be noticed, and for $MgB_{1.5}O_{0.5}$ it reaches E_b=-1.05984 Ry which is about 0.064 Ry higher than that of MgB_2.

The most energetically beneficial ordering was found to occur for the nearest (paired) oxygen atoms in the (001) type plains. The analysis of these data has shown that in the case of substitution of boron positions for oxygen the binding energy is essentially affected by the superlattice symmetry, the type of ordering of oxygen atoms and the amount of substituting oxygen atoms. In the case of 2×2×2 supercells, boron planes with and without substituting oxygen atoms alternate sequentially. The binding energy can decrease down to E_b=-1.13246 Ry or to E_b=-1.15268 Ry, i.e. below than that for MgB_2, and the substituting oxygen atoms located in the nearest positions form zigzag chains [21]. Thus the most preferable for the considered supercells is configuration when in the each boron plane (with partly oxygen substitution) the substituting oxygen atoms form zigzag chains and when the each subsequent boron plane contains only boron atoms at near pristine positions. As the calculations have shown [21], in the cases of the most preferable (from the energetic point of view) location of oxygen, when its amount is low, the shift of boron and magnesium atoms from the pristine positions (as compared with the case of ideal MgB_2 without substitutions) was not higher than 0.15 Å. It should be mentioned that results of high resolution TEM studies [22] indicate that oxygen atoms can be present regularly in every second boron plane of MgB_2. Thus in the practically undisturbed boron planes (from the point of view of binding energy and electron density distribution) there is still a possibility of high T_c superconductivity. Despite the fact that in the case of MgB_1O_1 chemical composition the formation of zigzag oxygen chains leads to even lower binding energy, E_b=-1.15712 Ry, and the amount of oxygen is so high that zigzag chains can be formed in each boron plane, such distribution in our opinion will be destructive for superconductivity, because each boron plane would be essentially distorted and the large deviations of Mg and B atoms from their pristine positions would take place. We suppose that such distribution of oxygen (zigzag chains in each boron plane) can be prevailed in the observed Mg-B-O nanolayers "L" or nanoinclusions "I" (figure 1c, d, f). This allows us to explain the tendency towards segregation of impurity O in MgB_2 structure during synthesis or sintering, and formation of Mg-B-O inclusions or nanolayers (with MgO type of structure), which effect pinning. So, seems the synthesis in the Mg-B-O system allows the realization of several phases with AlB_2 type crystal structure. Several (at least two) superconducting phases can be formed during crystallization with the structure of the same material due to the difference in melting temperatures of phases with different O content and the existing tendency for oxygen segregation. This makes it reasonable to perform analysis of such characteristic of MgB_2 as the two-band nature of the superconducting gap [1, 2] and 1.5 superconductivity (disorder of the vortex lattice) [23] in a new way.

In the case of $MgB_{2-x}O_x$ the lowest density of electronic states (DOS) about 0.46 states/eV/f.u. was found for $MgB_{1.75}O_{0.25}$ if the oxygen atoms are in neighboring positions [8]. If the concentration of oxygen is higher than in $MgB_{1.5}O_{0.5}$ the MgB_2 structure is destroyed. *Ab-initio* modelling of enthalpy of formation of boron substitution by oxygen in MgB_2 as well shows that this is energetically favourable up to the composition $MgB_{1.75}O_{0.25}$. . Enthalpy of MgB_2 formation is ΔH_f =-150.6 meV/atom and that of $MgB_{1.75}O_{0.25}$ is ΔH_f =-191.4 meV/atom. The formation of vacancies at the Mg site of both MgB_2 and substituted $MgB_{1.75}O_{0.25}$ was modelled as well, but has shown that such processes are energetically disadvantageous (ΔH_f of $Mg_{0.875}B_2$ and $Mg_{0.75}B_{1.75}O_{0.25}$ are equal to -45.5 and -93.5 meV/atom, respectively) [24].

For MgB_2 and $MgB_{1.75}O_{0.25}$ the calculations of the superconductive critical temperature (T_c) were performed within the framework of Density Functional Perturbation Theory (DFPT). First the calculations were performed on a low k-point mesh (8×8×8) to get the phonon dynamical matrices. After that the calculations of the McMillan-Allen-Dynes critical temperature T_c were performed on a high k-point mesh (16x16x16). Interesting, that the obtained T_c for the MgB_2 is 21.13 K, while for the $MgB_{1.75}O_{0.25}$ it is just a couple of degrees higher 23.3 K. It should be noted that it was hard to achieve the convergence of the phonon calculations for $MgB_{1.75}O_{0.25}$, which appeared to be unstable for the constructed supercells.

4. Conclusions

The experimental study and *ab-initio* modeling witnessed about the existence of superconductivity in *P*6/*mmm*, AlB_2 structural type $MgB_{1.75}O_{0.25}$. The level of superconducting characteristics (T_c, j_c in 0-10 T fields, B_{irr} and B_{c2}) of the materials with stoichiometry of the main phase $MgB_{1.8\text{-}1.68}O_{0.2\text{-}0.32}$ is the highest reported in literature. DFT calculations showed that B for O substitution in MgB_2 is energetically favorable up to $MgB_{1.75}O_{0.25}$. Other variants of substitutions and vacancy formations lead to less stable structure, which is in agreement with the results of Rietveld refinement. The calculated critical temperature T_c for $MgB_{1.75}O_{0.25}$ (23.3 K) is just a couple of degrees higher than for pure MgB_2 (21.13 K). The observed experimental T_c of the bulk MgB_2-based materials was 35.7-38.2 K. The advantages from location of substituted oxygen atoms in the nearby positions in the same boron plane allow explanation of the tendency towards segregation of impurity O in MgB_2 structure and formation of oxygen enriched areas which can affect pinning and critical current density increase.

5. References

[1] Bouquet F, Fisher R A, Phillips N E, Hinks D G and Jorgensen D 2001 *Phys. Rev. Lett.* **87** 047001
[2] Szabó P, Samuely P, Kačmarčík J, Klein T, Marcus J, Fruchart D, Miraglia S, Marcenat C and Jansen A G M 2001 *Physical review letters* **87**(13) 137005
[3] Jiang J, Senkowicz B J, Larbalestier D C and Hellstrom E E 2006 *Supercond. Sci. Technol. Rapid communication* **19**, L33
[4] Zhou S, Zhang Y, Pan A V, Dou S X, Chung K C, Kim Y K and Yoo J M 2009 *Supercond. Sci.*

Technol. **22**, 045018

[5] Prikhna T 2016 Structure and properties of bulk MgB_2 *Superconducting Wires: Basics and Applications* ed. R Fluekiger (World Scientific Series in Applications of Superconductivity and Related Phenomena 668 p) chapter 3a pp. 131-157

[6] Prikhna T A, Eisterer M, Weber H W, Gawalek W, Kovylaev V V, Karpets M V, Basyuk T V and Moshchil V E 2014 *Supercond. Sci. Technol.* **27**(4) 044013–044017

[7] Prikhna T A, Gawalek W, Savchuk Ya M, Sergienko N V, Moshchil V E, Wendt M, Habisreuther T, Dub S N, Melnikov V S, Kozyrev A V, Schmidt Ch, Dellith J, Litzkendorf D, Nagorny P A, Dittrich U, Sverdun V B, Kovalev L K, Penkin V T, Goldacker W, Rozenberg O A and Noudem J 2008 *Journal of Physics: Conference Series* **97**, 012022

[8] Prikhna T A, Romaka V V, Shapovalov A, Eisterer M, Sokolovsky V L, Weber H W, Grechnev G E, Boutko V G, Gusev A A, Kozyrev A V, Goldacker W, Podhurska V, Sverdun V.B, Habisreuther T, Schmidt Ch, Kovylaev V V, Shaternik V E, Karpets M V and Shaternik A V 2017 *IEEE Transactions on Applied Superconductivity* **27**, Issue: 4, 6200705 doi**:** 10.1109/TASC.2016.2638201

[9] Prikhna T, Eisterer M, Rindfleisch M, Ponomaryov S S, Tomsic M, Romaka V V, Moshchil V, Kozyrev A, Karpets M and Shaternik A 2019 *Journal of Superconductivity and Novel Magnetism* **31(**4) doi.org/10.1007/s10948-019-5062-z

[10] Prikhna T A, Eisterer M, Rindfleisch M, Kozyrev A V, Shaternik A V, Shaternik V E, Tomsic M, Moshchil V E, Karpets M V, Sverdun V B, Ponomaryov S S, Romaka V V and Seidel P P 2019 *IEEE Transactions on Applied Superconductivity* **29(**5) 1-5. doi: 10.1109/TASC.2019.2907662

[11] Bean C B 1964 *Rev. Mod. Phys.* **36** 31-36

[12] Pan A V, Golovchanskiy I A and Fedoseev S A, *Europhys.* 2013 *Lett.* **103**, 17006

[13] Golovchanskiy I A, Pan A V, Shcherbakova O V, and Fedoseev S A *J.* 2013 *Appl. Phys.* **114**, 163910

[14] http://www.wien2k.at/

[15] http://elk.sourceforge.net/

[16] Wills J M, Alouani M, Andersson P, Delin A, Eriksson O and Grechnev A 2010 Full-Potential Electronic Structure Method" *Energy and Force Calculations with Density Functional and Dynamical Mean Field Theory, Springer Series in Solid-State Sciences, Springer Verlag, Berlin* **167**

[17] http://fplmto-rspt.org/

[18] Barth von U and Hedin L 1972 *J. Phys. C* **5** 1629

[19] Perdew J P, Burke K and Ernzerhof M 1996 *Phys. Rev. Lett.***77**(18) 3865-3568

[20] Allen P B and Dynes R C 1975 *Phys. Rev. B*.**12**(5) 905 -922

[21] Prikhna T A, Shapovalov A P, Grechnev G E, Boutko V G, Gusev A A, Kozyrev A V, Belogolovskiy M A, Moshchil V E, Sverdun V B 2016 *Low Temperature Physics* **42** 380-394 doi: 10.1063/1.4952985

[22] Klie R F, Idrobo J C, Browning N D, Regan K A, Rogado N S, and Cava R 2001 *J Appl. Phys. Lett.* **79**, 1837

[23] Moshchalkov V, Menghini M, Nishio T,. Chen Q H, Silhanek A V, Dao V H, Chibotaru L F, Zhigadlo N D and Karpinski J 2009 *Phys. Rev. Lett.* **102**, 117001

[24] Prikhna T, Romaka V, Eisterer M, Shapovalov A, Kozyrev A, Grechnev G, Boutko V, Goldacker W, Habisreuther T, Vakaliuk O, Halbedel B 2017 *IOP Conf. Series: Materials Science and Engineering* 012023. doi:10.1088/1757-899

Acknowledgments

The investigations was performed in the frame of project III-3-18 (0776) supported by the National Academy of Sciences of Ukraine.